

Supplementary information

On-surface synthesis of ethers through dehydrative coupling of hydroxymethyl substituents

Yuyi Yan¹, Fengru Zheng¹, Zhiwen Zhu¹, Jiayi Lu¹, Hao Jiang¹, Qiang Sun^{1*}

¹Materials Genome Institute, Shanghai University, 200444 Shanghai, China

*Corresponding Author: qiangsun@shu.edu.cn

Contents

1. Additional results
2. Materials and Methods
3. References

1. Additional results

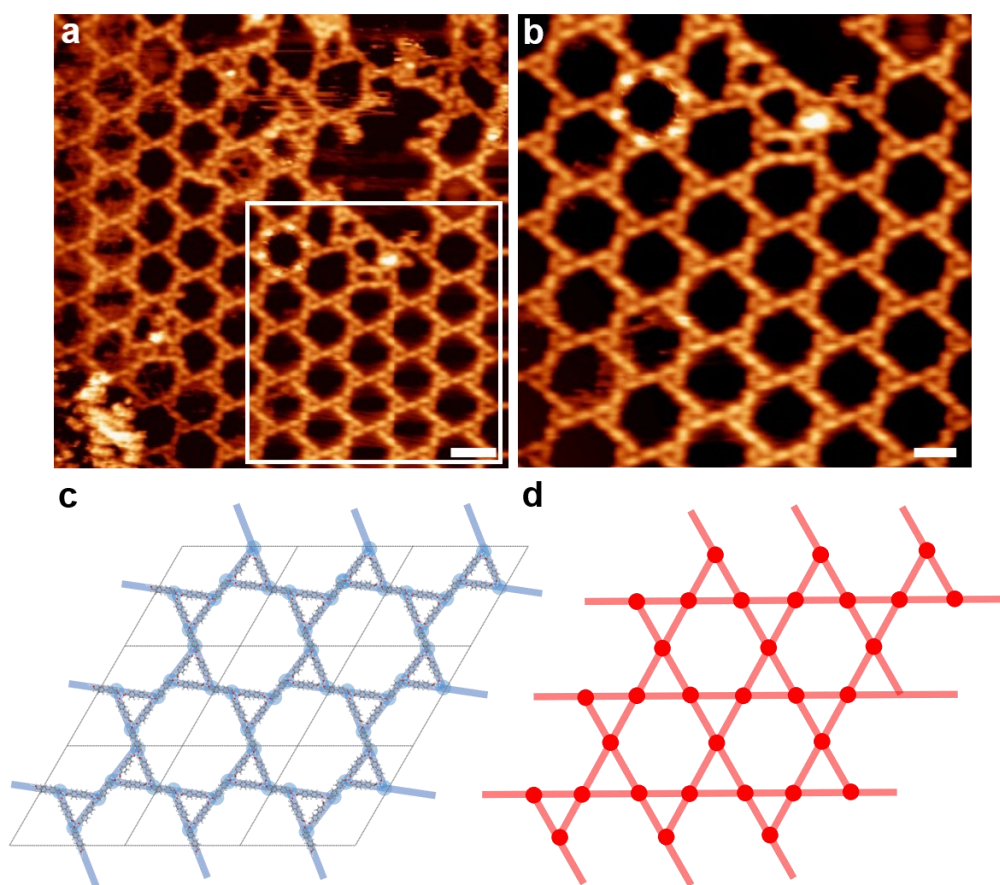


Figure S1. Kagome-like self-assembled pattern of molecule 1. (a) Large-scale and (b) close-up STM images showing the formation of the network structure after deposition of molecules **1** on Ag(111) held at RT. (b) is the zoomed area highlighted by a white box in (a). (c) Corresponding DFT model illustrating the self-assembled Kagome-like pattern and (d) Schematic diagram of Kagome lattice. (a) and (b) are acquired with $V_t = -1.8$ V, $I_t = 20$ pA. Scale bars: (a), 3 nm; (b), 2 nm.

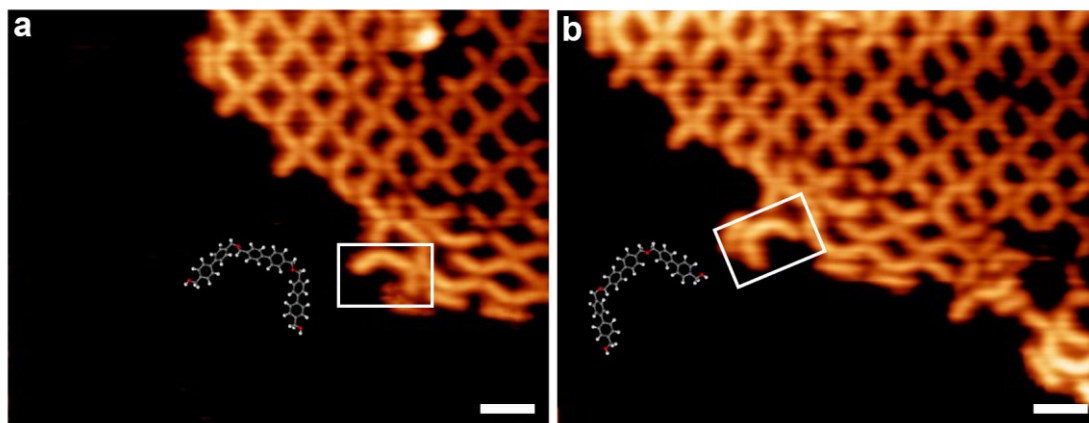


Figure S2. STM manipulation on an oligomeric ether. STM images (a) before and (b) after a lateral STM tip manipulation of a trimer structure highlighted by a rectangle, which provides strong evidence for the covalent nature of the oligomer. The corresponding structural models of the oligomer are shown beside the STM topographies of the oligomer. STM manipulation parameters: $V_t = -10$ mV, $I_t = 3.5$ nA. (a) and (b) are acquired with $V_t = -1.0$ V, $I_t = 50$ pA. All scale bars: 2 nm.

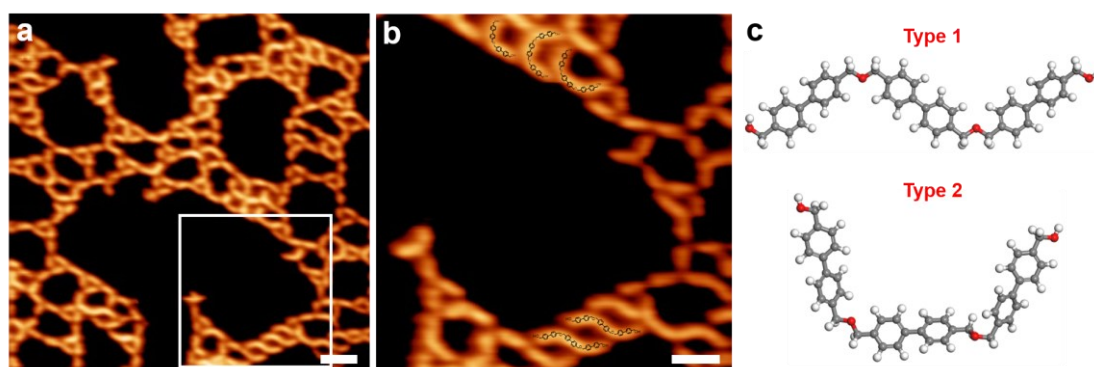


Figure S3. Two types of trimerized oligomers. (a) Large-scale and (b) close-up STM images showing two types of C-O-C bonded trimer structures with different configurations. The corresponding chemical schemes of the trimer structures are overlapped on some molecules in (b) for a better illustration. The region where (b) was imaged is indicated by the square in (a). (c) DFT optimized models of the two trimer structures. (a) and (b) are acquired with $V = -1.0$ V, $I = 100$ pA. Scale bars: (a), 3 nm, (b), 2 nm.

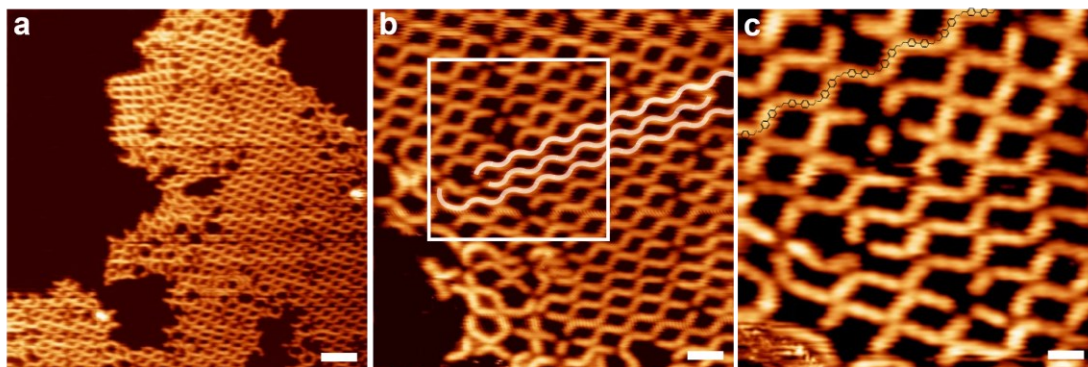


Figure S4. Additional STM images of the ether products on Ag(111) surface. (a) Overview and (b,c) zoom-in STM images showing the formation of one-dimensional ethers **2** with periodic C-O-C junctions on the surface. Some of ethers could extend a few tens of nanometers. The region where (c) was imaged is indicated by the square in (b). (a) and (b) are acquired with $V_t = -1.2$ V, $I_t = 50$ pA. (c) is acquired with $V_t = -0.1$ V, $I_t = 100$ pA. Scale bars: (a), 5 nm, (b), 2 nm, (c), 1 nm.

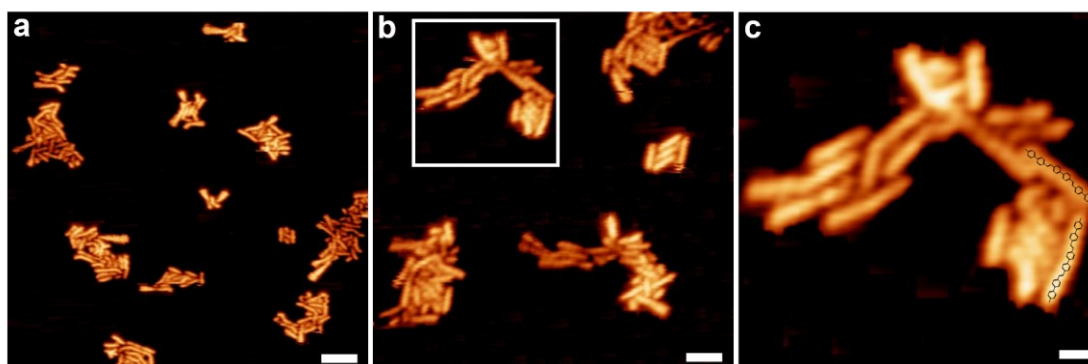


Figure S5. Additional STM images of product 3 on Ag(111) surface. (a) Overview (a) and zoom-in (b,c) STM images showing the formation of C-C coupled nanowires **3** on the surface. The region where (c) was imaged is indicated by the square in (b). (a), (b) and (c) are acquired with $V_t = -1.0$ V, $I_t = 100$ pA. Scale bars: (a), 5 nm, (b), 3 nm, (c), 1 nm.

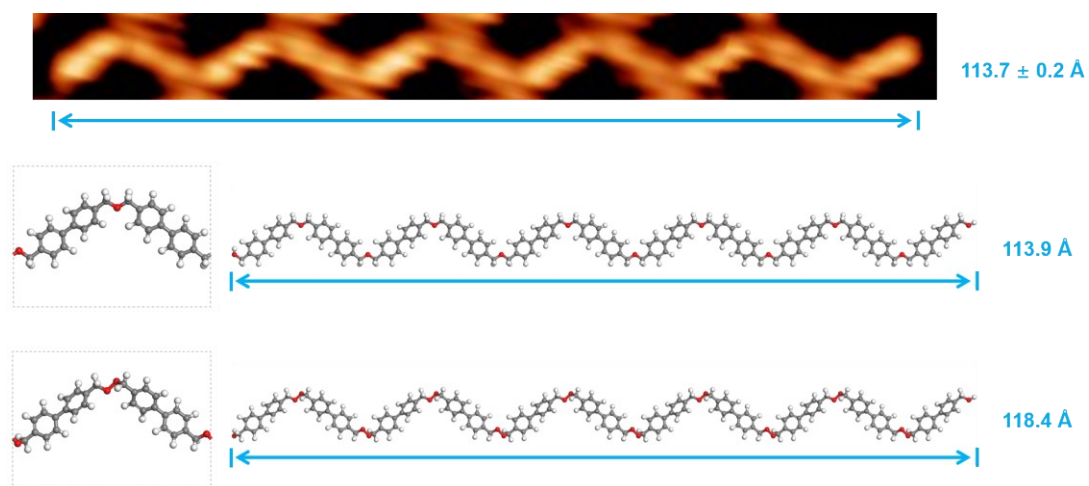


Figure S6. Confirmation of the C-O-C ether group. STM image of a zigzag undecamer. We have constructed and optimized the chain structures comprising the C-O-C (in the middle) and C-O-O-C (in the bottom) junctions, respectively. Their corresponding repeating units are shown on the left. The experimentally determined length of the undecamer is found to only agree with the C-O-C bonded ether chain.

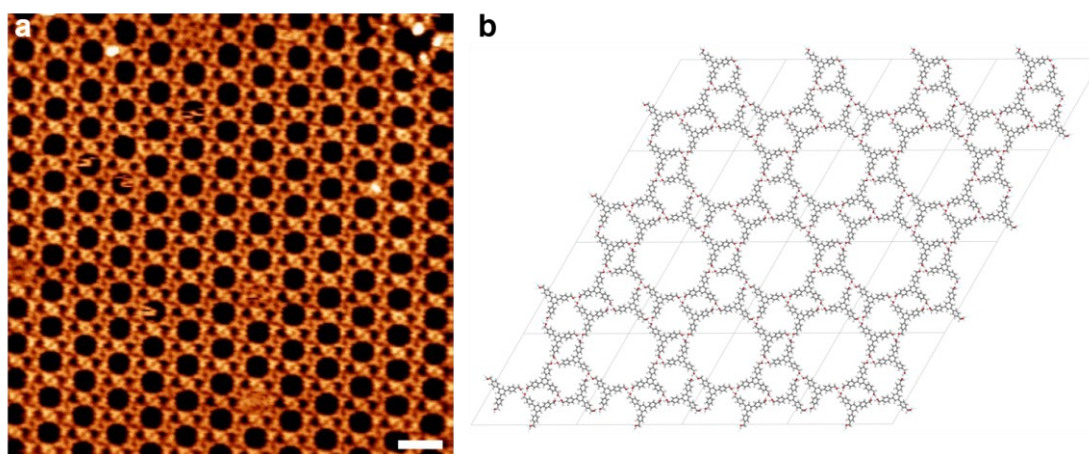


Figure S7. STM image of the self-assembled pattern of 4 on Ag(111) surface. (a) Large-scale STM image and (b) the corresponding DFT optimized model structure show the formation of a hexagonal porous pattern. The unit cell is indicated by lines in (b). (a) is acquired with $V = -1.2$ V, $I = 100$ pA. Scale bars: (a), 5 nm.

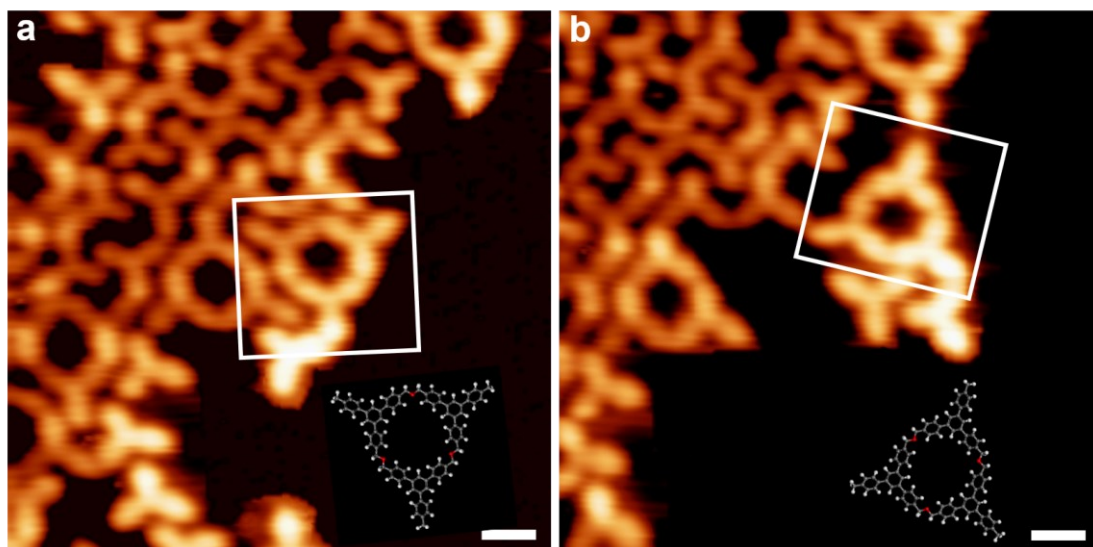


Figure S8. STM manipulation on an ether ring structure 5. STM images (a) before and (b) after a lateral tip manipulation of an ether ring which is highlighted by a white square, providing strong evidence for the covalent nature of the ring structure. The corresponding structural models of the ring structure are shown beside its STM topographies. STM manipulation parameters: $V_t = -10$ mV, $I_t = 3.5$ nA. (a) and (b) are acquired with $V = -0.5$ V, $I = 100$ pA. All scale bars: 1 nm.

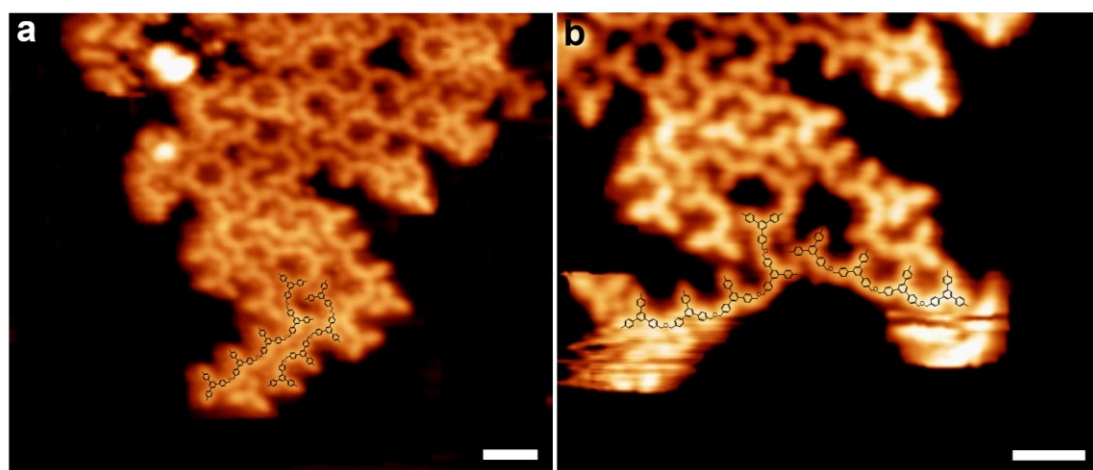


Figure S9. STM manipulation on the oligomeric chain structure formed by 5. STM images (a) before and (b) after a lateral tip manipulation of an ether chain, of which the chemical structures are overlaid on the STM images. STM manipulation parameters: $V_t = -10$ mV, $I_t = 5.0$ nA. (a) and (b) are acquired with $V_t = -0.5$ V, $I_t = 100$ pA. All scale bars: 2 nm.

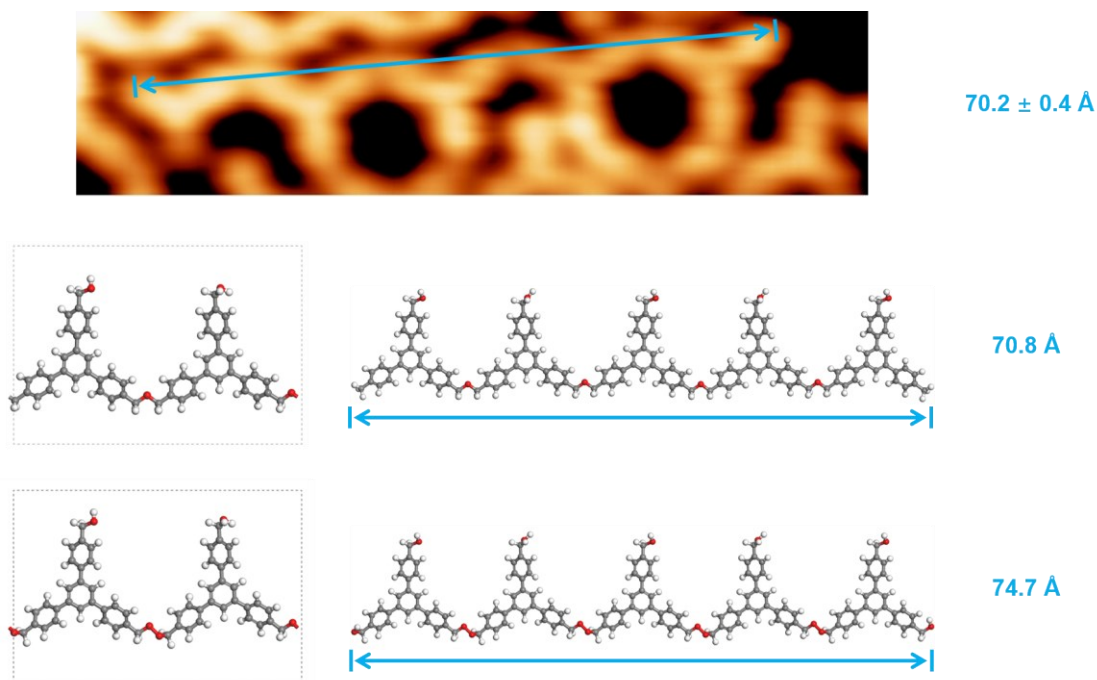


Figure S10. Confirmation of the C-O-C ether group in Fig. 3e. STM image of a pentamer formed by **4**. We have constructed and optimized the chain structures comprising the C-O-C (in the middle) and C-O-O-C (in the bottom) junctions, respectively. Their corresponding repeating units are shown on the left. The experimentally determined length of the undecamer only coincides with the C-O-C bonded ether chain.

2. Materials and Methods

STM characterization and sample preparation.

STM experiments were performed in a UHV system (base pressure 5×10^{-11} mbar) equipped with the low-temperature STM (Bosezi (Beijing) Co. Ltd. and Nanonis electronics), a molecular evaporator and other standard facilities for sample preparations. The metal substrates were prepared by several cycles of 1.5 keV Ar^+ sputtering followed by annealing at temperatures of around 800 K for 15 min, resulting in clean and flat terraces separated by monatomic steps. After the molecular evaporator was thoroughly degassed, the **1** and **4** molecules were sublimated from the molecular evaporator at 373K and 418K, respectively. The sample was thereafter transferred within the UHV chamber to the microscope, We used a resistive heating filament to anneal the samples. Temperatures to trigger reactions were controlled by a DC power supply and monitored by an infrared thermometer. All STM measurements were acquired at liquid nitrogen temperature (~ 78 K), and thermal treatments to trigger chemical

reactions were conducted for 30 minutes if not stated otherwise. The STM images were analyzed using WsXM.¹

Computational details.

The density functional theory (DFT) calculations are performed with the Vienna Ab Initio Simulation Package (VASP). Projector-augmented-wave pseudopotentials and the Perdew–Burke–Ernzerhof exchange-correlation functional were employed.^{2,3} Van der Waals (vdW) interactions were taken into account using the dispersion corrected DFT-D3 method of Grimme.⁴ All the structures were relaxed in DFT until residual forces on all unconstrained atoms were less than 0.03 eV/Å for geometry optimizations.

Charge density difference maps were computed by subtracting the charge densities of individual molecules from the total system $\Delta\rho = \rho_{\text{sys}} - \rho_{\text{A}} - \rho_{\text{B}} - \rho_{\text{C}}$.

We used the climb image nudged elastic band (CI-NEB) method to find the saddle point along energy paths between the reactants and products.⁵ The VASP transition state tools (VTST) was linked to the VASP package to allow for the CI-NEB method which has been proven to outperform the original NEB method implemented in VASP. We used the force-based Quick-Min optimizer to locate the saddle points.⁶ The reaction pathway optimization was stopped until the forces acting on the images along the path were converged to be less than 0.05 eV/Å. All the computations were carried out using the high-performance cluster at Shanghai University.

3. References

1. Horcas, I. *et al.* WSXM: A software for scanning probe microscopy and a tool for nanotechnology. *Review of Scientific Instruments* **78**, 013705 (2007).
2. Blöchl, P.E. Projector augmented-wave method. *Physical Review B* **50**, 17953-17979 (1994).
3. Perdew, J.P., Burke, K. & Ernzerhof, M. Generalized Gradient Approximation Made Simple. *Physical Review Letters* **77**, 3865-3868 (1996).
4. Grimme, S., Ehrlich, S. & Goerigk, L. Effect of the damping function in dispersion corrected density functional theory. *Journal of Computational Chemistry* **32**, 1456-1465 (2011).
5. Henkelman, G., Uberuaga, B.P. & Jónsson, H. A climbing image nudged elastic band method for finding saddle points and minimum energy paths. *The Journal of Chemical Physics* **113**, 9901-9904 (2000).
6. Sheppard, D., Terrell, R. & Henkelman, G. Optimization methods for finding minimum energy paths. *The Journal of Chemical Physics* **128**, 134106 (2008).